International Journal of Civil Engineering

Structure
Concrete

Experimental and numerical study on the effect of core shape and concrete cover length on the behavior of BRBs

A. Rahai[1,*], M. Mortazavi[1]

Received: May 2013, Revised: October 2013, Accepted: November 2013

Abstract

During the past years the use of buckling restrained braces (BRBs) have had a dramatic growth due to their better performance comparing to conventional braces. BRBs have more ductility and energy absorption capacity by excluding the overall brace buckling. However, even these kinds of braces have some problems restricting their use in some projects, i.e. high tolerance of applying unbonding material, concrete placing difficulties and their weight. Accordingly, many researchers have conducted experiments to find the possibility of shortening or even eliminating the infill material of the braces. The following study has addressed the effect of debonding material friction ratio, shortening the concrete fill, and finally eliminating it if possible, by reshaping the core element with constant section area. The operated analysis has been carried out both numerically and experimentally. ABAQUS finite element software was applied for numerical analysis and the results were verified by an experimental study in two groups of models each including four full-scale brace models. With a constant core section area, results revealed that without the risk of buckling, the concrete cover length could be reduced. With a special core profile, the infill may be fully omitted and the restrainer would be made up of only a steel tube, which may happen without any changes made to the cross sectional area of the core profile.

Keywords: *Finite element analysis, Buckling Restrained Brace, Restrainer cover, Hysteretic response, Optimum cover length, Tube shaped profiles.*

Notations

P_e: $Euler\ buckling\ load$
P_y: $yeild\ load$
S: $Gap\ between\ core\ and\ restrainer$
$B_{r,c}$: $width\ of\ restrainer\ tube, Core\ plate$
$t_{r,c}$: $thickness\ of\ restrainer\ tube, Core\ plate$
$t_{f,w}$: $thickness\ of\ flange, web\ (I-shaped\ profile)$
F_y: $yeild\ stress$
F_u: $ultimate\ stress$
E: $modulus\ of\ elasticity$
υ: $Poisson's\ ratio$
ε_u: $ultimate\ strain$

1. Introduction

Comparing with conventionally braced frames, Buckling Restrained Braced Frames (BRBFs) have the great advantage of yielding under both tension and compression without global buckling which leads the brace behavior to a symmetric and stable hysteretic response.

However, Buckling Restrained Braces have some disadvantages restricting their successful application in many countries.

During recent years, there have been some attempts to remove concrete infill or replace it with precast concrete panels.

** Corresponding author: rahai@aut.ac.ir*

1 Amirkabir University of Technology, Tehran, Iran

In this field, Watanabe (1988) estimated the optimum Pe/Py ratio in buckling restrained braces [1]. Chou (2010) suggested sandwiching the core plate between two restrainer elements using bolts [2]. Each restrainer element is made up of a precast concrete panel with a steel cover, which obviates the difficulties by unbonding material and placing concrete. Rahai (2009) surveyed the operation of various types of restrainer elements with a constant core profile, both numerically and experimentally [3]. They concluded that among restrainer types of steel tubes, PVC pipes and FRP sheets, braces with steel tube restrainers exhibit the best cyclic performance. Amadeo (2010) also proposed a type of BRB, which operates, based on yielding the restrainer walls [4]. This all-steel configuration is designed as two steel tubes in each other. The inner one, which is the core, is welded to the outer one

as a restrainer in some special parts causing the applied energy to be dissipated by yielding the restrainer wall in some certain areas. There has also been a discussion on the possibility of changing the yielding part of the core plate and its effect on hysteretic behavior by Mirtaheri (2011) [5]. Hoveidae (2012) conducted a parametric study on all-steel BRBs with different amounts of gap size (between the core and the restrainer element) and initial imperfections to investigate the global buckling behavior of such braces [6]. They concluded that the flexural stiffness of the restrainer element could affect the global buckling behavior of the brace and they also suggested a minimum ratio of the Euler buckling load of the restraining member to the yield strength of the core, Pe/Py for design purposes. The effect of gap size on BRB's fatigue performance has been studied as well by Usami (2011) [7]. All-steel BRBs proposed by Jun-Hei (2009) were manufactured using a steel bar as a load-resisting core member and a hollow steel tube as restrainer to prevent global buckling of the core [8]. The gap infill for the braces was steel bars or mortar as fillers. The performance of the two different types of braces was compared by uniaxial and subassemblage tests.

The results indicated that the performance of the BRB with discontinuous steel bars as filler material was not satisfactory, whereas the BRBs with continuous bars or mortar filler showed acceptable performance. Takeuchi (2012), proposed a strategy for the prevention of in-plane local buckling failure of a BRB whose restrainer is composed of a mortar in-filled circular or rectangular steel tube with various mortar thicknesses [9]. They reconstituted the criteria necessary to prevent in-plane local buckling failure. There are some recent investigations on applying different alloys to improve the hysteretic response of BRBs (Miller (2012) [10], Wang (2013) [11]).

In addition, there have been some literature reviews on the research and application of BRBs in different countries. Uang (2004) and Xie (2005) have presented a summary of various types of BRBs all over the world ([12] & [13]).

The present study addresses the possibility of reducing the concrete cover or eliminating it. This survey is carried out by analyzing some experimental and numerical models described below. The numerical models were debated in four groups. The core profile of each group is initially exposed to special loading and the results are contrasted to the ones obtained from the complete BRB. The loading system is both uniform and cyclic load. Consequently, there are two series of experimental models. Each series consists of four full-scale models exposed to cyclic loading and eventually the obtained results are contrasted.

2. Proposed Models

2.1. Introduction

As previously mentioned, the models are designed to survey the effect of unbonding material friction ratio, concrete cover length and its elimination, core profile shape and to determine the optimum restrainer dimensions when the concrete cover is removed. The following analyses conducted are Eigen value buckling analysis, nonlinear buckling analysis, and dynamic explicit analysis. The models are introduced in four groups:

- Group A

This group consists of four models each formed of a core profile, concrete cover and a steel tube (Fig. 1). There is a gap, S, to permit lateral deformation of the core profile. An imperfection of 0.5S is also introduced to all specimens. The difference between the four models is the unbonding material friction ratio. This ratio differs as 0, 0.1, 0.2, and 0.3 for models A1 to A4. The constituent materials are steel for core plate and restrainer tube and concrete as the cover infill and unbonding material between core plate and concrete fill.

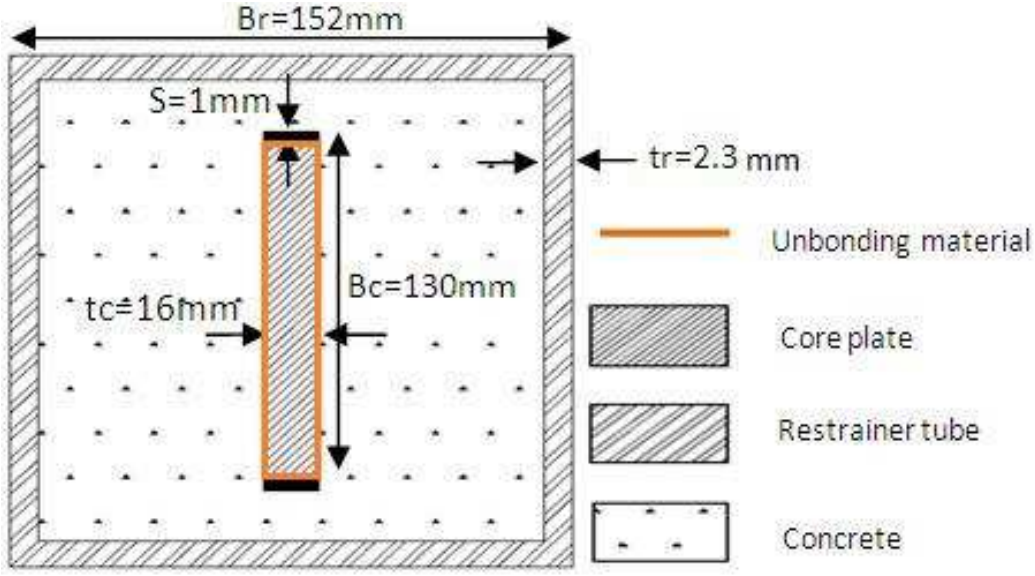

Fig. 1 cross section of group A

The total configuration of the braces considering the boundary conditions is illustrated in Fig. 2. As it is described in the next section, instead of modeling the detailed connections, half of the plastic core length is considered rigid on both sides of the core (Takeuchi (2010) [14]).

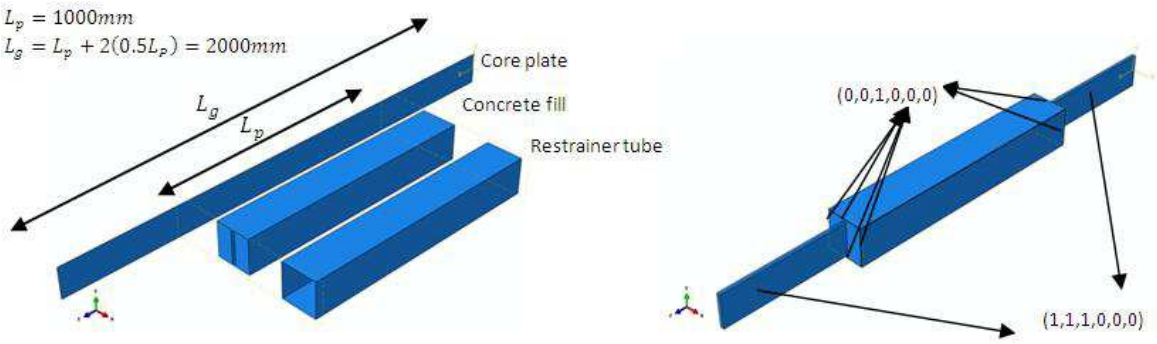

Fig. 2 overall schematic of group A of models

- Group B

The fundamental components of the models of this group are the same as group A, considering cross section dimensions and boundary conditions (Figs. 1, 2). The difference between models of this group is the restrainer element length. The restrainer length varies in the models but the core plastic length remains constant. The friction ratio among the models is considered equal to zero. The cover length in models B1 to B5 varies as 500mm, 650mm, 700mm, 750mm, and 1000 mm.

- Group C

There are four models here; three models (C1 to C3) include restrainers with concrete infill and the last one (C4) is restrained just by a steel cover. The core profile in this group of braces is configured as a compacted I shaped profile. The general scheme of the braces of this group is shown in Fig.3. Models C1 to C3 are analyzed to observe the effect of the gap between core and concrete fill and the way it is applied. Model C4 with a core profile similar to other models of this group demonstrates the behavior of the brace without any infill material as a restrainer. The boundary conditions are considered similar to other groups and more details are given in Table 1.

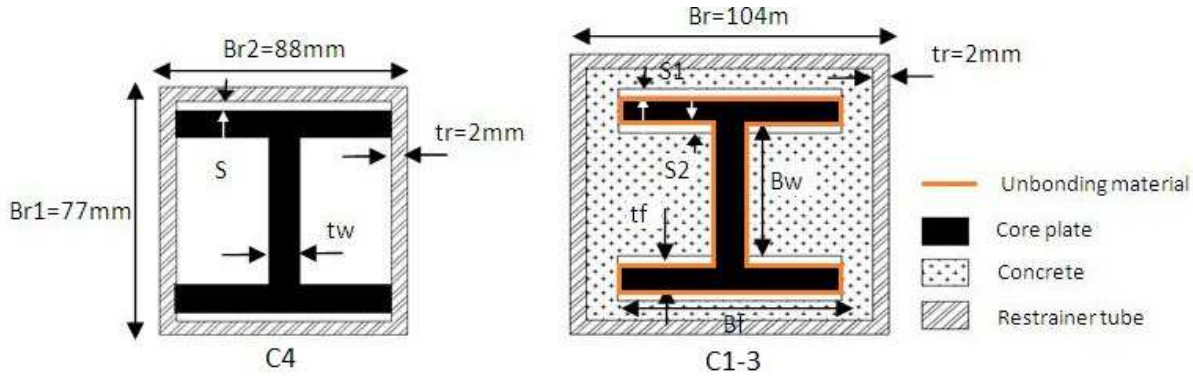

Fig. 3 cross section of group C

Table 1 Detailed dimensions of models of group C

	I shaped core dimensions				Gap size	
Specimen	Bw(mm)	Bf(mm)	tw(mm)	tf(mm)	S1(mm)	S2(mm)
C1	50	84	11	7.5	0.5	0.5
C2					1	0
C3					0.5	0
C4					1	

- Group D

The last group of braces is designed in a way that the concrete fill is eliminated. Each specimen consists of a steel core covered by a steel restrainer (Fig.4). Excluding the concrete fill, it is necessary to change the core shape in a way that the steel tube can singly restrain its buckling. Therefore, the core profile is changed from a plate to a box shaped profile with the same cross sectional area. This group consists of 10 models with the same core dimensions. The distinction among the models is the dimensions and the thickness of the restrainer tube. These

dimensions vary in a way that models D1 and D2 possess the inner core tube while regarding the rest of the models; the core profile is the outer tube. This group of models is designed to evaluate the possibility of eliminating the cover infill in BRBs. Restrainer thickness is the only variable between D1 and D2 and the response of the braces with the inner core tube is surveyed. Between D3 and D4, braces with an outer core tube, the restrainer tube thickness is the only changing parameters. In models D5 to D7, the effect of the gap between core and restrainer on the cyclic behavior of the braces is studied. Models D8 to D10 are designed with the same purpose but in higher restrainer thicknesses. The boundary conditions are considered similar to other groups.

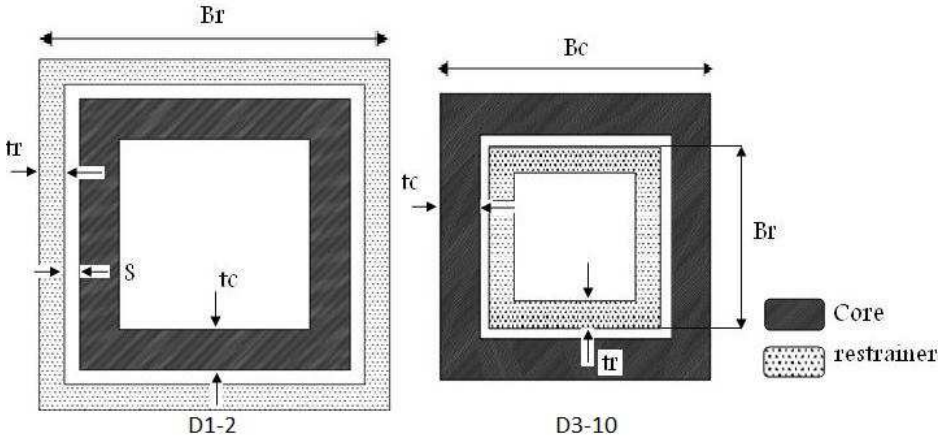

Fig. 4 cross section of group D

As it is demonstrated in Table 2, the Pe/Py ratio in most of the models is less than 1.5, as determined by AISC.

Table 2 Detailed dimensions of models of group D

specimen	Br (mm)	tr (mm)	Bc (mm)	tc (mm)	S (mm)	P_e/P_y
D1	77.6	1.3	73	8	1	1.337
D2	79	2	73	8	1	2.11
D3	55	1.3	73	8	1	0.466
D4	55	2	73	8	1	0.689
D5	55.6	1.3	73	8	0.7	0.481
D6	56	1.3	73	8	0.5	0.492
D7	57	1.3	73	8	0	0.520
D8	56	2.3	73	8	0.7	0.824
D9	55	1.4	73	8	1	0.499
D10	56	1.4	73	8	0.5	0.527

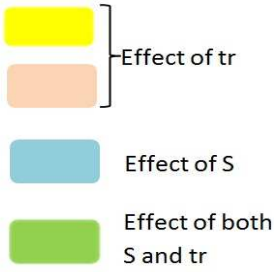

2.2. Material properties

The applied materials consist of steel as core and restrainer tube, concrete, and unbonding material. The unbonding material is not introduced as an independent material but its effect is considered as a friction ratio in the contact elements.

2.2.1. Steel

The steel behavior is introduced as a bilinear behavior as represented in Table 3. The combination of kinematic and isotropic hardening behavior of steel and the role of isotropic hardening of steel has been previously pointed out (Lopez-Almansa (2012) [15] , Zona (2012) [16]). However, here the hardening model is considered fully kinematic (Takeuchi 2010 [14]).

Table 3 Steel properties

	Plastic behavior			Elastic behavior	
	F_y(Mpa)	F_u(Mpa)	ε_u	E(Gpa)	υ
core	280	480	10	205	0.3
restrainer	351	510	15	205	0.3

2.2.2. Concrete

There is a Concrete Damaged Plasticity model to define the confined concrete behavior. This model is

applied in this study because the infill concrete satisfies the conditions of confinement (Table 4).

Table 4 Elastic and plastic properties of concrete

Elastic properties		Plastic properties				
E (N/mm^2)	v	Delation angle	eccentricity	fb/fc	K	viscosity
26480	0/167	1	0/1	1/16	0/667	0

Compressive failure		Tensile failure	
Fracture parameter	Plastic strain	Fracture parameter	Cracking strain
0	0	0	0
0.1299	0.0004	0.3	0.0001
0.2429	0.0008	0.55	0.0003
0.3412	0.0012	0.7	0.0004
0.4267	0.0016	0.8	0.0005
0.5012	0.002	0.9	0.0008
0.566	0.0024	0.93	0.001
0.714	0.0036	0.95	0.002
0.8243	0.005	0.97	0.003
0.9691	0.01	0.99	0.005

2.3. Variety of applied elements

To model the concrete, the C3D8R element, belonging to ABAQUS library, with the approximate dimensions of 40mm is used which is the reduced shape of C3D8. In the case of the thin walled core profile and restrainer, the shell element is selected. The S4R shell element with dimensions of 20×20mm is applied. A sensitivity analysis is carried out to select the optimum element size. The error percent for various element sizes versus the run time for each of them is provided in a curve; the intersection point demonstrating the optimum element size (Fig.5). Modeling the interaction between core and restrainer tube, the Surface-to-Surface type of contact element with appropriate friction ratio and hard contact normal behavior is considered. The interaction between concrete and steel cover is defined as a tie to constrain all transitional degrees of freedom.

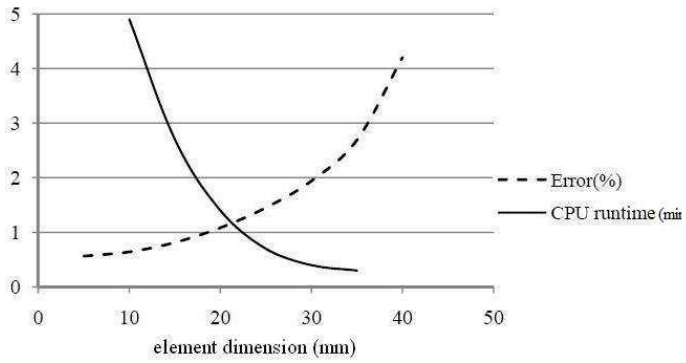

Fig. 5 determination of optimum element size

3. Verification

Takeuchi (2010) proposed a method of modeling the BRBs in which the concrete infill is omitted and only its effect is considered by determining some special boundary conditions. There are some details about this method presented in the following section, then braces with exactly the same assumptions are modeled and analyzed and finally the obtained results are compared to that of the referred article to be the base of the next analysis on the proposed BRBs in future studies.

When the effect of the concrete fill between the edge of the core and restrainer wall is negligible, two plates from the top and bottom (Fig.6) may restrain the local buckling of the core. The boundary condition on the edge of the plates should be fixed to consider the effect of concrete infill on the restrainer walls. This effect on the core plate is provided by boundary conditions restraining core rotation and displacement around its weak axis.

According to the introduced method of modeling, the brace is modeled as depicted in Fig.6. The results and its comparison with the referred study are provided in the next section. The next step then would be to check if the simplified method of not modeling the concrete fill gives a correct answer. In this regard, the brace is also modeled once considering the concrete infill and the attained results are compared to the ones of the mentioned simplified method. According to the referred article, the exerted load is determined as a cyclic displacement control loading with cycles of ±0.1%, ±0.5%, ±1%, ±2% and ±3% of core plate strain.

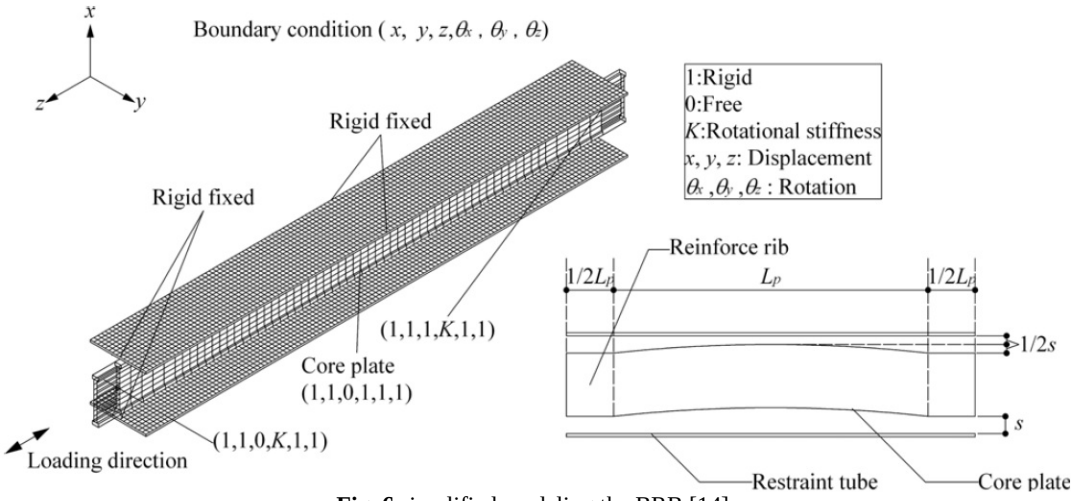

Fig. 6 simplified modeling the BRB [14]

3.1. Verification results

The hysteretic curves of the above-mentioned models are presented as Fig.7-a (the red curve). The horizontal parts of the numerical and experimental curves (bold and dashed curves), are steeper than the one for the obtained curve. The reason is that the hardening behavior is defined as fully kinematic which in reality is a combination of kinematic and isotropic behavior, but due to the suggestion of the authors of the article referred to previously (Takeuchi (2010) [14]), the error would be negligible if the hardening is considered as fully kinematic. The hysteretic curve of the original model and the simplified one (the one without modeling the concrete fill) are provided in Fig.7-b. It can be observed that the two curves almost match each other demonstrating that the simplifyied method gives acceptable results. The desirable adaption of two curves (original numerical model and verification model) could be judged comparing their cumulative plastic deformation during the load cycles, presented in Table 5.

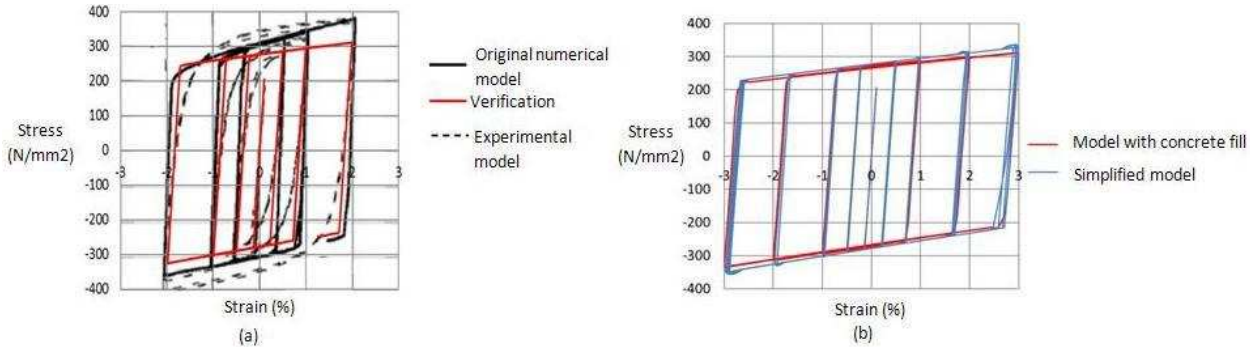

Fig. 7 comparing obtained hysteretic response of numerical, experimental and verification analysis

Table 5 Comparing cumulative plastic deformation between numerical and verification models

	numerical model original	model verification
cycle load	cumulative plastic deformation	
three cycles first 0.5% of strain	33.94	31.38
three cycles second 1% of strain	80.71	77.59
three cycles third 2% of strain	170.39	166.43
∑	285.04	275.4

4. Analysis Results

Using the verified method, the four groups of introduced models are analyzed and the results are evaluated as below.

4.1. Individual core behavior

For a better recognition of their behavior, the individual cores of the braces are initially modeled and analyzed using linear and nonlinear buckling behavior. Table 6 provides the buckling load in the first 10 modes of buckling, under Eigen value analysis.

Table 6 Buckling load for the first 10 modes

Group D		Group C		Groups A and B	
Mode	Buckling load (kN)	Mode	Buckling load (kN)	Mode	Buckling load (kN)
1	9346.74	1	5076.8	1	354.33
2	9346.74	2	7101.46	2	722.97
3	17093.18	3	7857.77	3	1416.48
4	17093.18	4	9894.37	4	2139.41
5	24127.74	5	10400	5	3182.66
6	24136.58	6	10403.9	6	41490.05
7	24495.38	7	10653.3	7	5623.28
8	24539.84	8	10680.2	8	7010.64
9	25107.42	9	11071.6	9	8686.34
10	25231.96	10	11156.5	10	9592.83

Considering the imperfection applied in linear buckling analysis, the first mode shape of the core plate would be initially applied to the models. The nonlinear analysis with uniform compressive loading would be applied to the individual core profiles to attain the force-displacement curves. These curves have been presented in Fig.8 for all different core profiles. In the case of plate core profile, the load in which the curve breaks to a horizontal trend, would be the buckling load and in the box and I-shaped profiles, it would be the yielding load exactly after which core buckling happens. Fig.9 demonstrates the buckling load charts attained by different analysis methods. As it was expected, due to inelastic buckling occurrence in box and I-shaped core profiles, the buckling load resulting from linear analysis is not an exact answer and generally differs from the ones resulting from nonlinear analysis. In the next step, the core profile of each group is imposed on the introduced cyclic loading to provide a comparison between the cyclic behavior of the individual core and a complete BRB. As Fig.10 illustrates, buckling happens in the plate core profile by the 0.1% strain and this shows low energy dissipation capacity. As it was estimated because of low moment of inertia in one direction, the core buckles around the weak axis in a low amount of force. However, the core with box and I-shaped profiles under higher amounts of force, first yielded and then buckled.

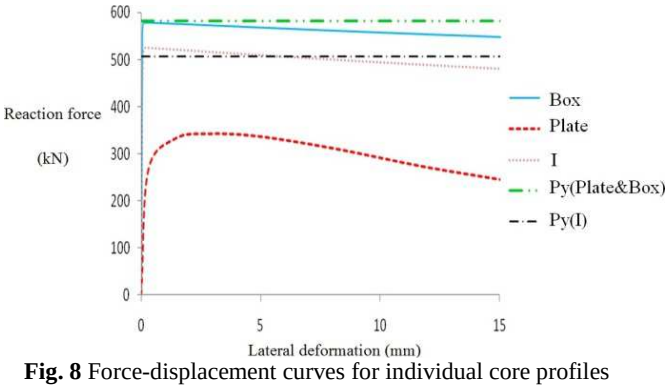

Fig. 8 Force-displacement curves for individual core profiles

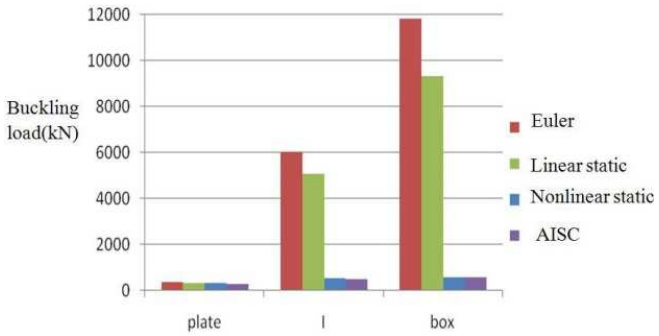

Fig. 9 Buckling load charts attained by different analysis methods

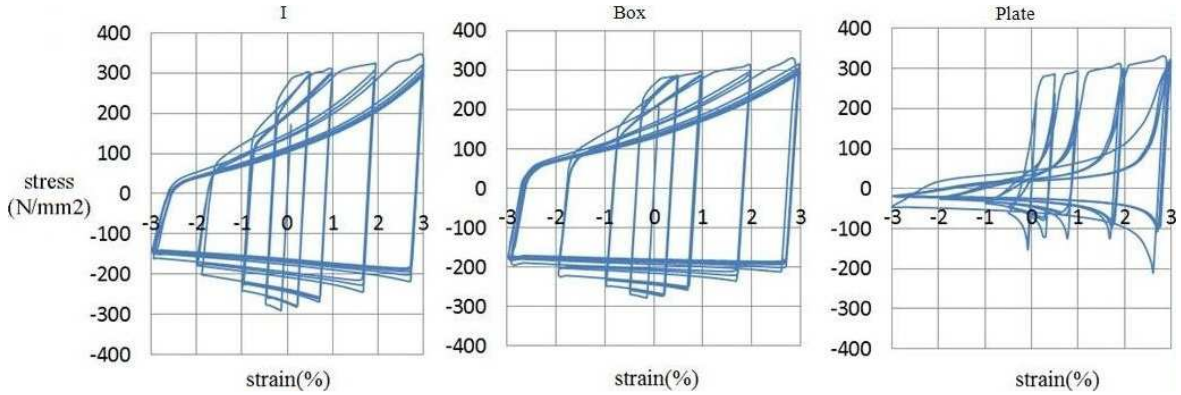

Fig. 10 Hysteretic response of individual core profiles

4.2. Covered brace performance

To evaluate the brace behavior, the previously introduced cyclic load is applied to the proposed models. The obtained results are classified as follows.

- Group A

The resultant hysteretic curve of models of group A are presented in Fig.11. It is seen that increasing the friction ratio up to 0.3 does not affect the overall hysteretic loops, but causes an increase in maximum compressive load in some cycles. To control this increase, there is a β factor introduced by AISC, which is defined as below (Eq. (1)):

$$\beta = \frac{P_{compressive}}{P_{tensile}} \tag{1}$$

For all models of group A, the amount of β factor is provided in Table 7. According to AISC (2005) [17], the maximum allowable amount of this factor is 1.3; therefore, all models of A1 to A4 are in a permissible range.

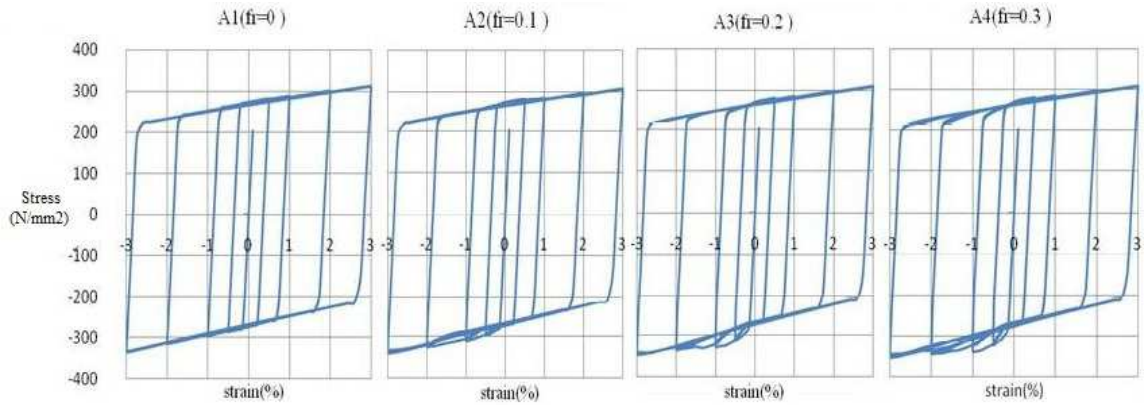

Fig. 11 Hysteretic response of models of group A

Table 7 β factor for models of group A

Model	A1	A2	A3	A4
β	1.071	1.107	1.150	1.194

The maximum load resisting capacity in each cycle indicates the brace ability to resist axial loads. Fig.12 illustrates the maximum compressive and tensile capacity of the braces in each group.

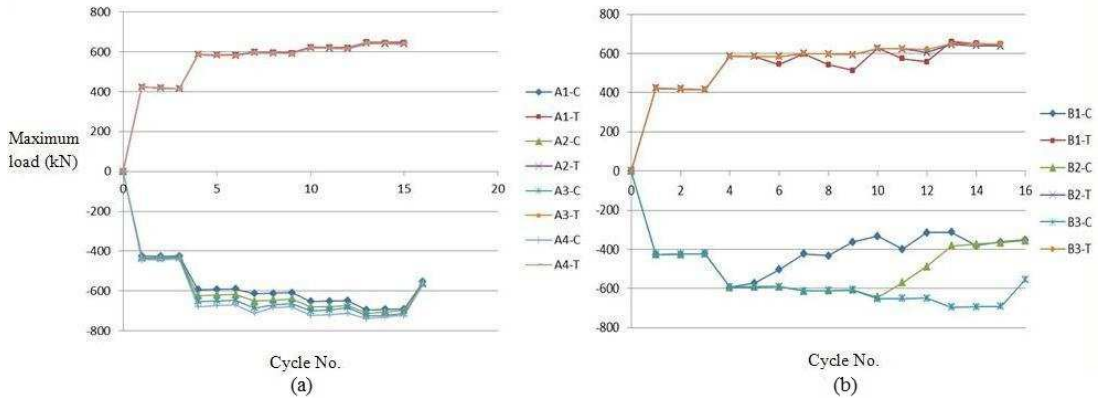

Fig. 12 maximum load in each cycle for models of: (a) group A, (b) group B

Another parameter presented here is the lateral deformation of the core of braces shown in Fig.13. The lateral deformation of the A1core profile is symmetric along the brace but for others with some friction between core and restrainer, the formed peaks are pulled to the direction of the fixed support (Fig.13). The lateral deformation near fixed support has developed severe fluctuations in a short length but according to the curves, it did not cause any instability in the brace cyclic performance until it reached a friction ratio of 3%.

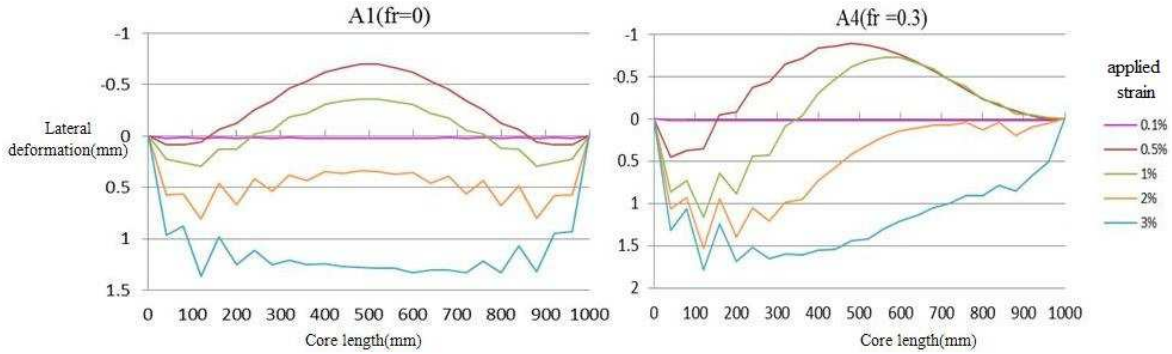

Fig. 13 lateral displacement of core plate

- Group B

In this group of models, the optimum cover length is worked out without any change in core section. This length is the shortest length in which there is no buckling occurring in uncovered parts. Operating nonlinear static analysis, it was revealed that in braces B3 and B4 with the cover length of 700mm and 750 mm, no buckling was observed. In the case of braces B1 and B2, along the uncovered parts, local buckling occurred. Fig.14 illustrates how the cores of braces B1 to B3 deform while buckling occurs. Fig.15 also illustrates how the hysteretic behavior of braces is affected by cover length reduction.

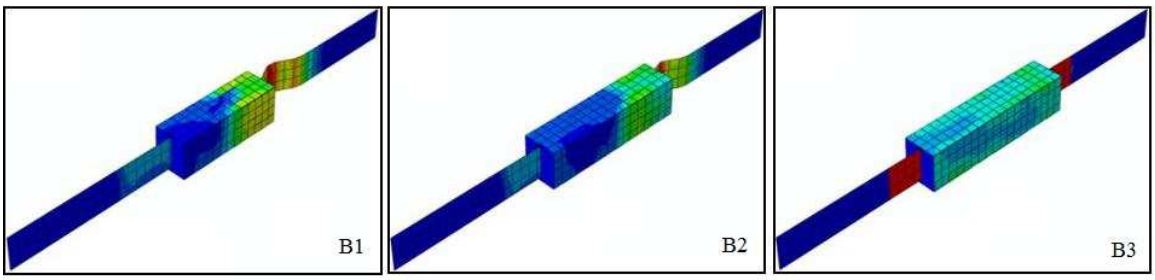

Fig. 14 Core buckling in models of group B

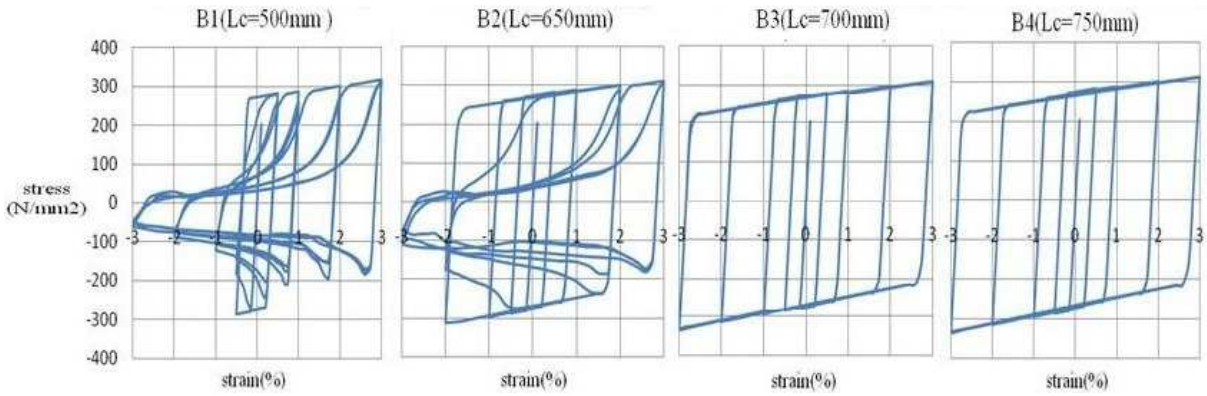

Fig. 15 Hysteretic response of models of group B

Curves of Fig.15 demonstrate that reducing the cover length down to 0.7 times the initial cover length does not cause any significant change in brace hysteretic response. Shortening the cover to half its initial length (B1) caused buckling in the fifth cycle (0.5% of core strain) which indicates a dramatic loss of energy dissipation capacity. Model B2, having 35% of reduction in the cover length, is buckled by the 10th cycle (2% of core strain).

Fig.12-b compares the maximum load resisting capacity of models B1 and B2, which have unsymmetrical hysteretic responses, to B3 with a symmetric response in spite of its reduced cover length. The decline in load capacity of braces B1 and B2 is obvious compared to model B3.

- Group C

As previously mentioned, models C1 to C3 include concrete infill and C4 is an all-steel model. The resultant hysteretic responses are illustrated in Fig.16.

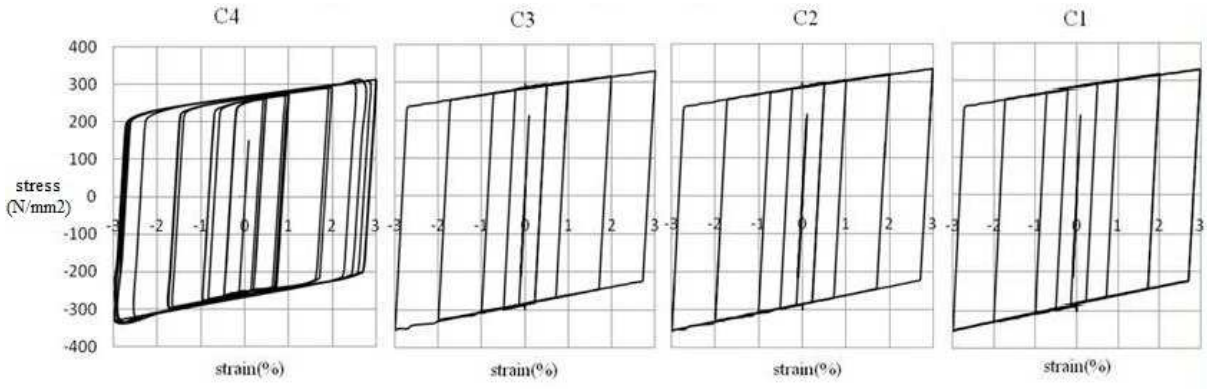

Fig. 16 Hysteretic response of models of group C

All models with concrete infill (C1 to C3) represented stable hysteretic responses. C4 also had a symmetric and stable hysteretic curve. The lateral deformation of the cores with 15 times magnification is shown in Fig.17. The local buckling of flanges in all models can be observed in this figure. The web buckles about its strong axis in models C1, C3, and C4, which is desired for dissipating energy. Because of the hollow space between flanges, in the case of models without concrete fill (C4), the flange plate crushed inside.

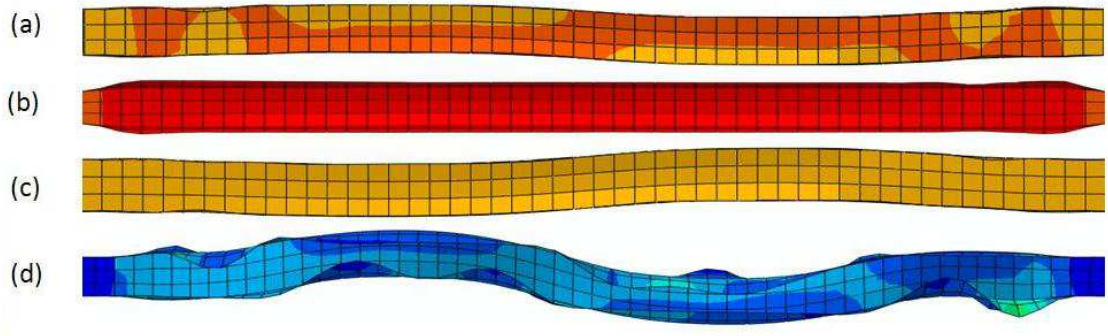

Fig. 17 lateral deformation of the cores with 15 times magnification: (a) C1, (b) C2, (c) C3, (d) C4

- Group D

This group of models aims to survey the possibility of reducing the concrete infill, without any increase of core or restrainer tube cross section area. A core section of rectangular shape is not suitable for the mentioned goal because it is not feasible to design a steel cover fitting such a core without any infill material. In addition, there must be a thickness of infill material in such cases around the weak direction to prevent its buckling about the weak axis. Therefore, it would be appropriate to consider a core profile with exactly the same cross section area and equal moment of inertia about both axes in order to eliminate the need of restraining it in a special direction. In this case, the steel cover may have a symmetric shape and restrain the buckling of the core in each direction symmetrically. Initially, to evaluate the compressive strength, the models are subjected to uniform compressive load and their axial and lateral deformation is provided in front of the reaction force in a curve (Fig.18).

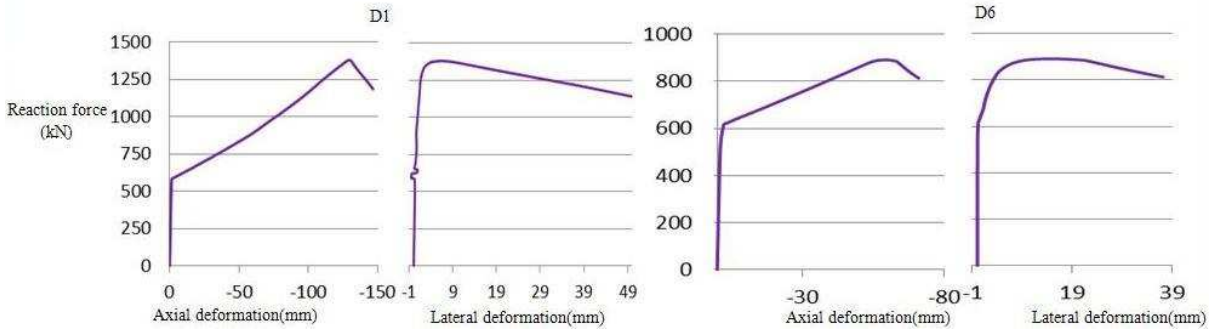

Fig. 18 Axial and lateral deformation in front of the reaction force

Fig.18 demonstrates that when the core yields and buckles under the 600kN of force immediately afterwards, the axial displacement- reaction force curve continues the upward trend with a lower but constant slope as benefiting well from the post buckling capacity. In the curves referring to models D1 and D2, the maximum force goes

higher than the failure force of 1000kN. This is because once the buckling occurs, the core contacts the restrainer and the buckling transfers from the first mode to higher modes of buckling, each wall of the core box also buckles locally which causes some energy dissipation. There is a comparison between maximum load capacities of models with inner restrainer in Fig.19. Based on this diagram, the maximum load resisting capacity is not exactly in direct relation to Pe/Py ratio. Increasing this ratio generally increases the maximum load resisting capacity; but comparing D4 and D10 clearly shows different results. This is because there is another effecting factor of S. Regarding the models with inner restrainers, the cyclic behavior was expected to be improved by reducing the gap, S, because by pressing the core box, its inner perimeter expands and the core wall deviates from the restrainer wall. Therefore, in this case it was estimated that the smaller gap sizes give a better response. Comparing models D3 and D5 to D7, reveals that reducing the S size from 1mm to zero did not help in any way. Nevertheless, regarding models D9 and D10 with just 0.1mm of increase in restrainer thickness, the effect of gap reduction is obviously visible. By reducing S from 1mm to 0.5mm, without any considerable change in Pe/Py ratio, both hysteretic and compressive responses improved.

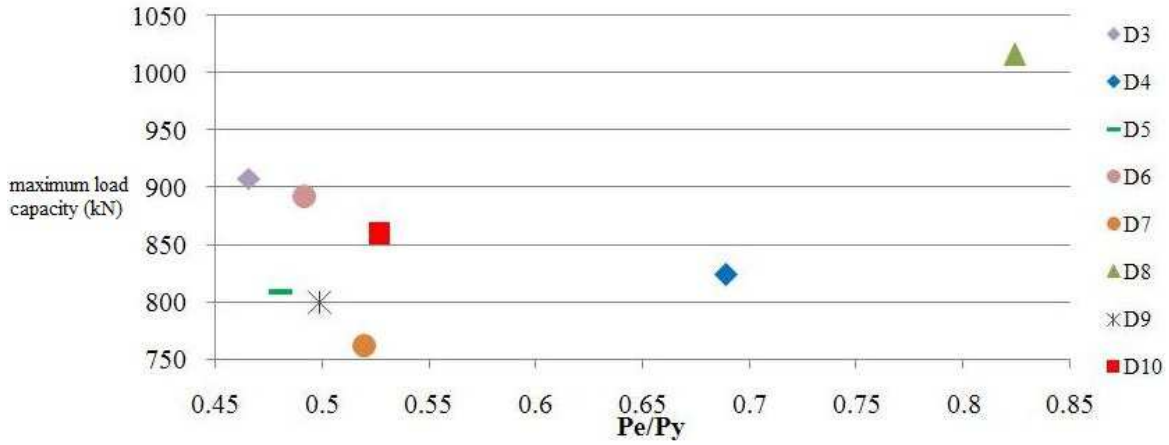

Fig. 19 maximum compressive strength of group D

Finally, each of the models of group D are subjected to cyclic loading, the hysteretic response in some case would be instable for core strains of higher than 2% (Fig.20). As it can be observed, the curves referring to models D3 and D5 to D7 show buckling occurrence in strain amounts of lower than 3%. Models D1 and D2 in which the restrainer is the outer tube, responded

desirably. Between the models with inner restrainer, models D4, D8, and D10 did not experience buckling and had a stable hysteretic response. Except for the gap size between the core and restrainer, all other dimensions remain constant among models D3 and D5 to D7. The restrainer thickness remained constant between models D3 and D1 to check the effect of the core and restrainer position, as inner or outer tube, on brace behavior. Fig.20 shows that model D3 with S size of 1mm and restrainer thickness of 1.3mm had an instable response. As it was mentioned, this brace response is expected to be improved by reducing the gap size; in this case, models D5 to D7 with the same conditions of D3 but a different S were analyzed but also did not respond as a stable curve. Considering the suitable response of model D4 with a 2mm thickness and 1mm gap, it is estimated that with a thickness between 1.3 to 2mm and gap size of less than 1mm, an acceptable response may be attained. Therefore, models D9 and D10 with restrainer thickness of 1.4 mm were designed and analyzed. D9 had an unstable response with a 1mm gap size (Fig.20) but by decreasing it to 0.5mm in D10, the response clearly improved and an ideal hysteretic response was obtained.

For a better comparison between the buckling models with D1, which is the one with an ideal response, their maximum load resisting capacities are presented in Fig.21. It is concluded that among models with inner restrainer tube, models with a Pe/Py ratio less than 0.53, buckle in strain ranges of lower than 3% and represent less compressive strength. Among the models with a constant restrainer thickness of 1.3mm, D3 exhibited the most inappropriate response and in the 14th cycle, while applying the first cycle of 3% strain, a dramatic strength loss occurred. Reducing the gap size to 0.7mm in D5 and 0.5mm in D6 improved the behavior to the 15th and 17th cycle respectively but did not prevent buckling. Model D7 with a core tube fixed to the restrainer without any gap, also did not give a better response. This means that the restrainer thickness is insufficient to prevent buckling. By just a 0.1mm increase of restrainer thickness and a gap size of 1mm in model D9, the brace resisted the whole loading process and did not fail but the strength loss started at the 14th cycle. With the same dimensions, reducing S to 0.5mm in D10 gave a perfect response without any strength loss or buckling occurring until the 18th cycle.

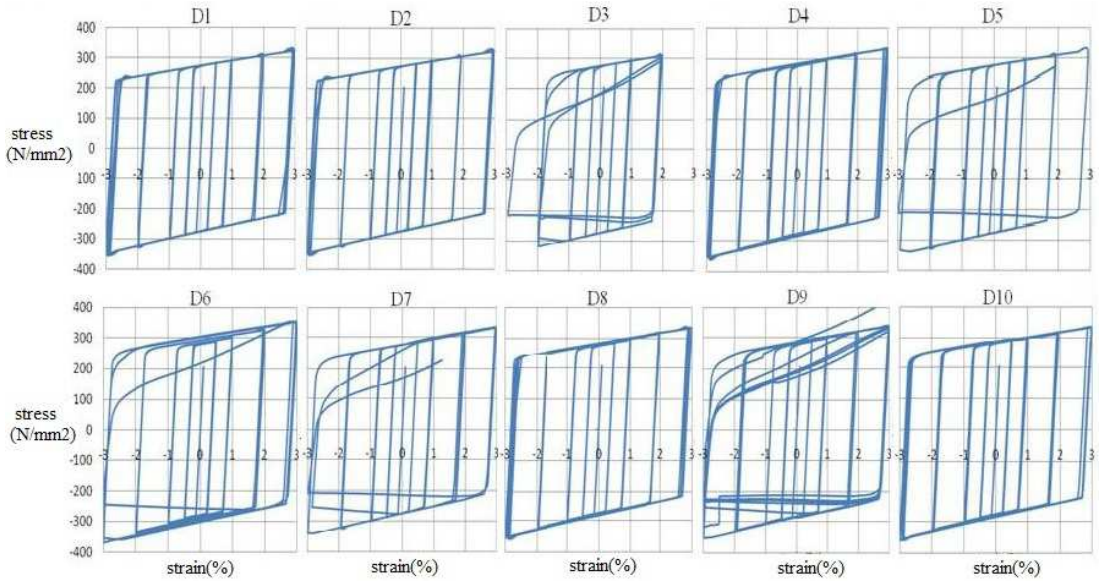

Fig. 20 Hysteretic response of models of group D

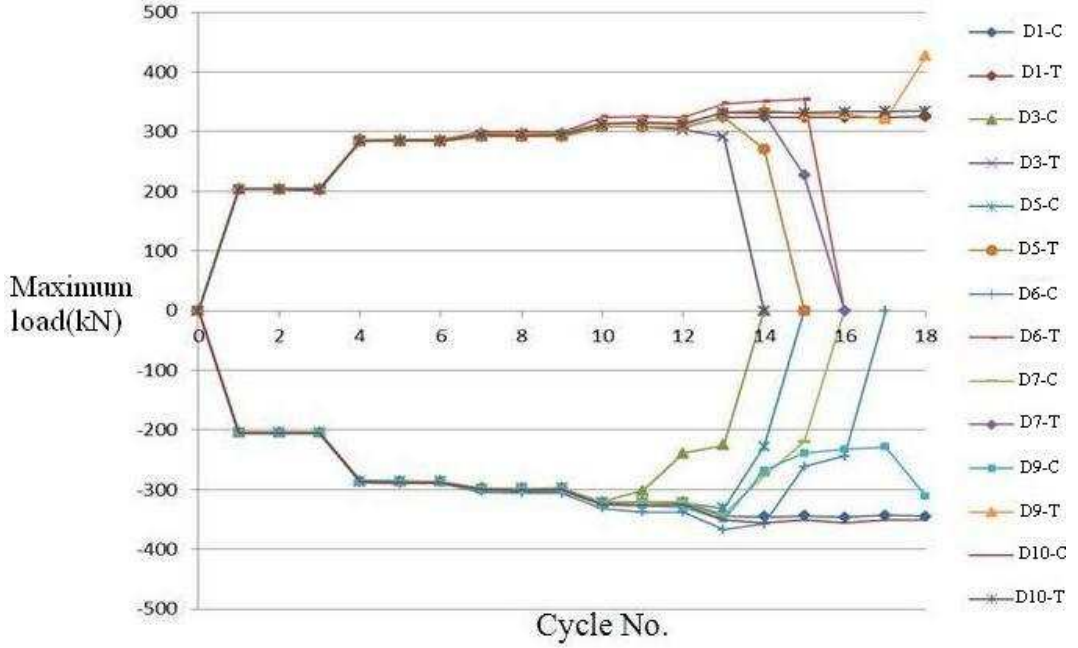

Fig. 21 maximum load in each cycle

5. Experimental Study

According to the shape of the core profile in the last group of models having a box shaped section, the core behavior of this kind, as a closed section needs to be evaluated accurately to determine possible difficulties. Therefore, two series of full-scale experimental models are defined to be subjected to axial cyclic loading. This experimental study is conducted to help the analytical results be more reliable and safe. The loading system consists of a Servo test jack with nominal loading capacity of 1000 KN, a rigid floor, and the holding frame. The Servo test jack is capable of displacement control loading. The loading protocol introduced to the jack is a displacement control sinusoidal cyclic load with the amplitudes mentioned in section 3 and a frequency of 0.01 Hz.

5.1. Introducing experimental specimens

In this study, there are two series of specimens, of which the characteristics and details of performing experiments are given below.

5.1.1. First series of specimens

To fabricate the first series of specimens, the D2 model from the numerical analysis is selected because it had a stable hysteretic curve up to 3% of core strain. Four full-scale Buckling Restrained Braces were initially constructed. As it is illustrated in Fig.22, each specimen is made up of a core box, a restrainer tube (conforming D2), two base plates for up and down connections, 8 gusset

plates to fix the elastic part of the core as it was estimated to be in numerical studies. One specimen among the four is selected to be the control used to evaluate the unpredictable difficulties. The specimens are named as D2-1 to D2-4.

Fig. 22 General Configuration of experimental specimens

Since the connections are not previously modeled in numerical analysis, to construct the first specimen, some dimensions are selected for connections of the control sample to observe its behavior. Fig.23 represents the details of the experimental specimens; all dimensions except t_1 and t_2 are constant in all of them.

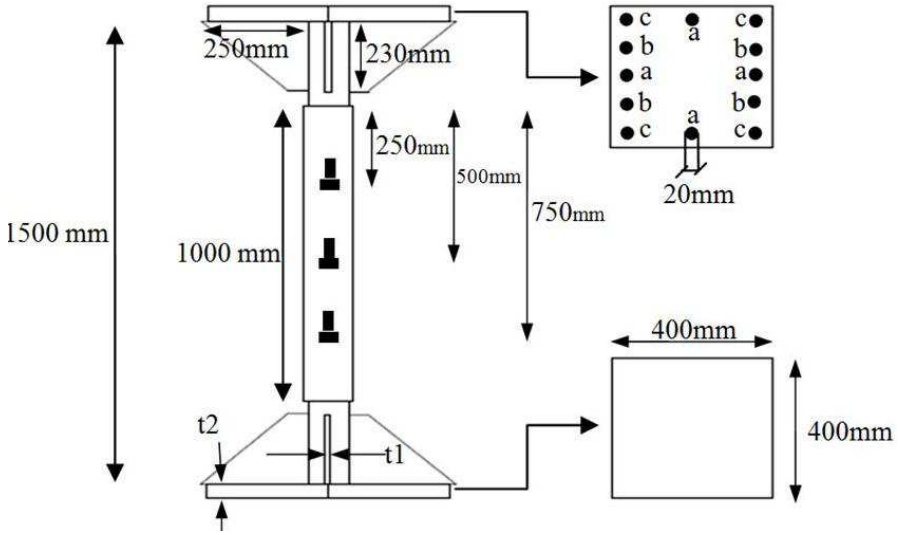

Fig. 23 details of the experimental specimens and dimensions

Since the core is hidden under the restrainer and is not visible, to observe how the buckling happens, some strain gauges are attached to the restrainer cover. According to the unpredictable buckling direction, the strain gauges are attached on two perpendicular walls of the restrainer. The attachment points are on the 250mm, 500mm, and 750mm height of the restrainer wall and in two horizontal and vertical directions. Fig.24 illustrates the overall configuration of the braces and their strain gauges by details.

The results of the tests are as follows:

- specimen D2-1

In this specimen, the connection plate thickness is 10mm and the gusset plate thickness is 8mm. The lower plate is welded to a rigid floor and the upper one is connected to the jack with four bolts of 20mm diameter in the holes of series “a”, as shown in Fig.23. After starting the loading process, the first six cycles were completed without any problems but by starting the 7th cycle, the upper plate had considerable deformations near the connected bolts and almost no deformation was exerted to the core profile. Fig.25 clearly shows the sagged part near the connecting bolt. Generally, the applied displacement to the core did not reach the yield point of the core box. The force-displacement curve of model D2-1 is shown in Fig.26. By adding a force higher than 60 KN and applying 12 cycles of loading, no specific buckling is observable. Only at the end of the 12th cycle, the change of the curve slope shows the buckling occurrence.

Fig. 24 Experimental set up and the position of strain gauges

Regarding the weakness of the upper plate under tension, in the next specimens, the plate thickness increased to 30mm and the gusset plate"s thickness to 15mm.

In the case of the other three specimens of D2-2 to D2-4, the loading was carried on to the 13th cycle, and the loading system did not show the capacity to apply loads higher than 60 tons so that the displacements were exerted less than the determined amount.

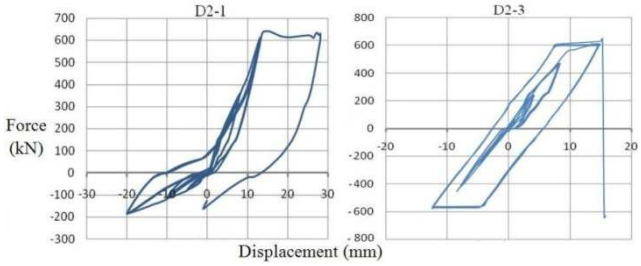

Fig. 26 Force-displacement curve of models D2-1 and D2-3

Fig. 25 Sagged plate near the connecting bolt

Since the two specimens D2-2 and D2-4 are fabricated similar to each other, the obtained results generally match. The results for model D2-3 are presented in Fig.26 as an example. It is demonstrated that the loading cycles of 10mm displacement are applied as 8mm and the ones with 20mm of displacement are applied as 15mm.

Opening the restrainer wall of specimen D2-3 and observing its core plate demonstrates the core buckling under the second mode, which is clearly shown in Fig.27.

Fig. 27 Core buckling under the second mode

5.1.2. Second series of specimens

The second series of specimens was designed with a smaller cross section area and therefore, lower buckling load. They are designed so that the individual core buckles under the introduced loading, but in the presence of the restrainer element, the buckling would be eliminated. The $\frac{KL}{r}$ ratio is also kept constant and equal to that of the specimens of the first series. The cross sectional area is considered almost half of the first series. In this regard, five different profiles were selected and analyzed in order to determine their hysteretic behavior and pick out the best choice for the next series of experimental studies. The evaluated profiles are box shaped and their details are provided in Table 8. According to the obtained results, profile E with the dimensions of $70 \times 70 \times 5$ was selected and its hysteretic response both as an individual core and as a restrained brace is represented in Fig.28.

Table 8 Determination of a new profile for experimental studies

profile	$I(mm^4)$	A	r(mm)	$P_e(kN)$	$F_e(\frac{N}{mm^2})$	L(mm)	$\frac{L}{r}$	$F_{cr}(\frac{N}{mm^2})$	$P_{cr}(kN)$
A: $60 \times 60 \times 4$	459000	882	22.81	3714.71	4211.69	800	35.07	272.32	240.18
B: $60 \times 60 \times 5$	541000	1080	22.38	4378.35	4054.02	800	35.74	272.02	293.78
C: $70 \times 70 \times 3.2$	627000	846	27.22	5074.35	5998.05	1000	36.73	274.58	232.3
D: $70 \times 70 \times 4$	753000	1040	26.91	6094.08	5859.69	1000	37.16	274.45	285.43
E: $70 \times 70 \times 5$	896000	1280	26.46	7251.38	5665.14	1000	37.8	274.27	351.06

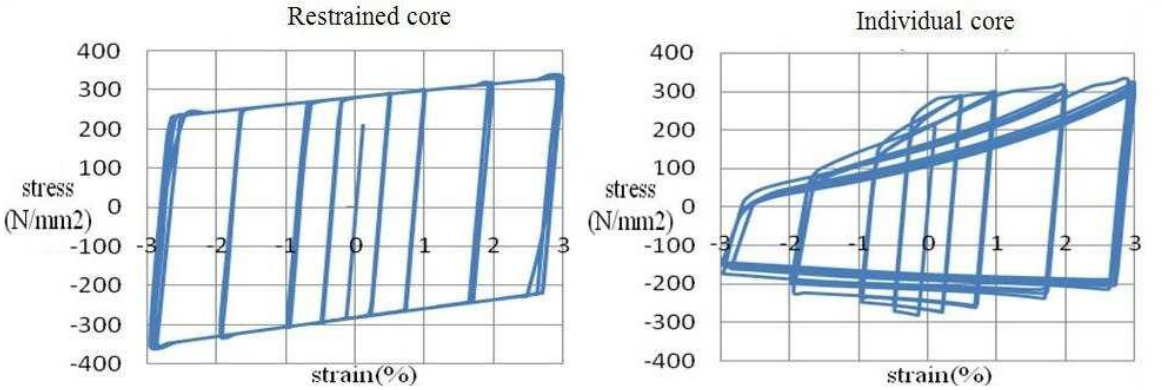

Fig. 28 Hysteretic response of profile E both as individual and restrained core

The general composition of these four specimens named E1 to E4 is similar to the first series of models. The only variables are t_1 and t_2 (Fig.23) which are changed in the connection. As a result of core thickness reduction, the end plate and gusset plate thickness are also reduced to 15mm and 8mm, respectively.

- Observations and results

The first three models (E1 to E3) are constructed uniformly. E4 also consists of a similar core, but it is tested in the absence of the restrainer wall to evaluate the effect of the restrainer element. The load- displacement curve for model E2 is represented in Fig.29 as an example. It demonstrates that during the 9th to 12th load cycles, the exerted displacement is about 16mm. There are some fluctuations in the forces of higher than 200kN, which are caused by weld cracking. Finally, the loading process stopped due to the failure of the welds of the lower plate to the rigid floor under tension. The force-displacement curve for model E4 as an individual core box is shown in Fig.29. This model failed by buckling as it was expected and the test stopped on the 7th cycle.

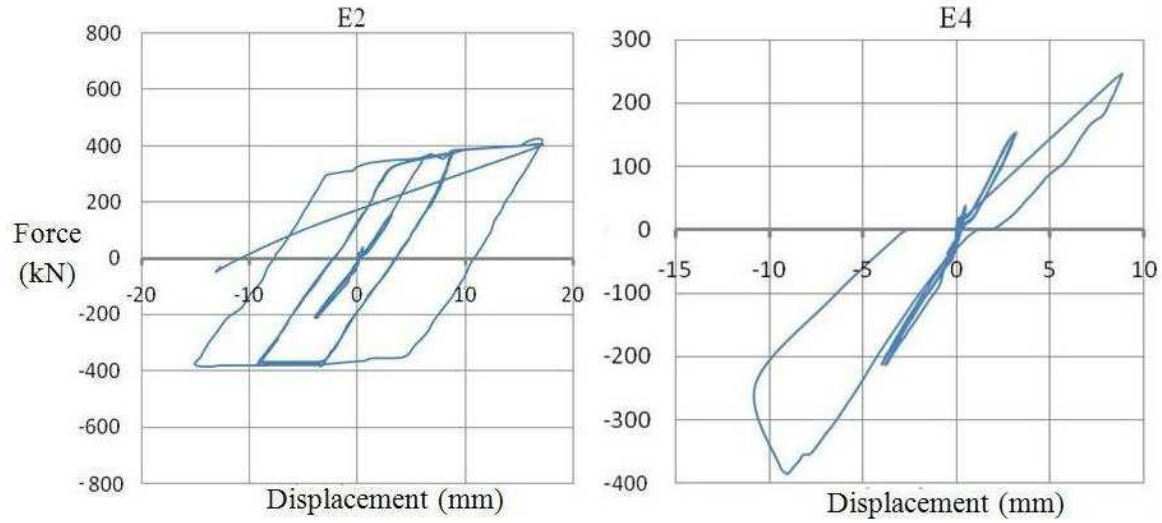

Fig. 29 Force-displacement curve for models E2 and E4

6. Conclusions

This paper aims to evaluate the optimum conditions for the cover element of the BRBs. The concrete applied as an infill for the restrainer cover, in addition to its heavy weight, possesses some special problems. In order to overcome these problems, this study initially attempts to survey the effect of friction ratio between core and concrete fill; then the cover length is reduced with no change in core section area and the effect of this reduction is observed. Finally, by changing the core profile to a box shaped profile with a constant section area, the suitable conditions for eliminating the infill material are provided and the models of all-steel BRBs are analyzed.

The conclusions are classified to the groups of surveyed models as follows:

- In the first group of braces, the major investigation is the effect of the unbonding material friction ratio and the following results are obtained:

- Increase in friction ratio between core profile and concrete surface, raises β up to about 1.2 in the braces of this group. However, the hysteretic curves remain stable and symmetric. It is concluded that up to 3% friction ratio keeps the braces in a permissible range of added resistance ratio, β.

- The problem caused by high friction ratio between core and concrete fill is the asymmetrical lateral displacement of the core in higher core strains, which may cause problems in the brace stability. However, due to the results attained in this study, it does not have any considerable effect on brace stability.

- Analyzing the second group of models which was designed based on optimum cover length, revealed that:

- The restrainer length can be reduced considerably without any increase in the cross section of the core profile. In this case, the optimum cover length is 0.7 times the core plastic length. This means that 15% of the core length projects from two sides of the restrainer. According to its short length, without any risk of buckling, this projection reaches the yielding point and dissipates the kinetic energy. It must be noted that the provided dimensions are reliable for the proposed braces of this study.

- Considering the models of group C, it can be concluded that:

- In the cases that the core profile consists of plates with a free edge (not a closed section), eliminating the concrete fill may cause those plated to crush inside the hollow space between flanges. However, generally eliminating the concrete fill did not have any negative impact on the hysteretic response of braces with I shaped core profiles.

- Discussing the models of group D with the approach of proposing an all-steel BRB gave the following results:

- Considering a core section with an equal moment of inertia about both axes, the required conditions to eliminate the concrete infill would be provided. This would also increase the buckling load as much as the yield loads.

- The increase in buckling load shifts the elastic buckle in the case of core plates to plastic buckling, while the core profile is box shaped. This would increase the brace load resisting capacity. The core plate initially yields and then buckles immediately. At this time, the restrainer operation starts and it restrains the first mode of buckling to the higher ones; also, the local buckling happens in each wall of the core box in higher strains. This operation leads to a maximum energy dissipation capacity about the proposed BRBs.

- Using the restrainer with the same thickness as an inner tube reduces its dimensions. Considering its acceptable performance, this would be a suitable change in this group of BRBs. However, as shown in this study, it is weaker than BRBs with an outer restrainer while applied to uniform compressive loads.

- The conditions of the gap size, S, in BRBs with restrainers as the inner tube differs from the ones with the outer tube. In this configuration, applying the compressive load increases the gap between core and restrainer. Therefore, the gap size in these types of BRBs may be considered as lower amounts compared to the ones with usual configuration.

- The all steel BRBs, with an outer restrainer tube resulted in acceptable hysteretic and compressive responses in Pe/Py ratios of higher than 1.3. In the case of braces with inner restrainer, the symmetric and stable hysteretic response is attained by the Pe/Py ratios of higher than 0.52, which is much lower than the limit determined by AISC.

- The experimental studies also verified the attained results and helped to prevent unpredictable observation such as crushing the box walls.

References

[1] Watanabe A, Hitomi Y, Yaeki E, Wada A, Fujimoto M. Properties of brace encased in buckling-restraining concrete and steel tube, Proceeding of 9th World Conference on Earthquake Engineering, Tokyo-Kyoto, Japan, 1988, IV, pp. 719-724.

[2] Chou CH, Chen SH. Subassemblage tests and finite element analyses of sandwiched buckling restrained braces, Journal of Constructional Steel Research, 2010, No. 8, Vol. 32, pp. 2108-2121.

[3] Rahai A, Alinia M, Salehi S. Cyclic performance of buckling restrained composite braces composed of selected materials, International Journal of Civil Engineering, 2009, No. 1, Vol. 7. pp. 1-8.

[4] Amadeo B. A brace-type seismic damper based on yielding the walls of hollow structural sections, Engineering Structures, 2010, No. 4, Vol. 32, pp. 1113-1122.

[5] Mirtaheri M, et al. Experimental optimization studies on steel core lengths in buckling restrained braces, Journal of constructional steel research, 2011, No. 8, Vol. 67, pp. 1244-1253.

[6] Hoveidae N, Rafezy B. Overall buckling behavior of all-steel buckling restrained braces, Journal of Constructional Steel Research, 2012, Vol. 79, pp. 151-158.

[7] Usami T, Wang C, Funayama J. Low-cycle fatigue tests of a type of buckling restrained Braces, Procedia Engineering, 2011, Vol. 14, pp. 956-964.

[8] Jun-Hei P, Jinkoo K. Cyclic test of buckling restrained braces made of steel rod and hollow steel tube, The 5th International Symposium on Steel Structures, March 12-14, 2009, Seoul, Korea.

[9] Takeuchi T, Hajjar JF, Matsui R, Nishimoto K, Aiken ID. Effect of local buckling core plate restraint in buckling restrained braces, Engineering Structures, 2012, Vol. 44, pp. 304-311.

[10] Miller DJ, Fahnestock LA, Eatherton MR. Development and experimental validation of a nickel–titanium shape memory alloy self-centering buckling-restrained brace, Engineering Structures, 2012, Vol. 40, pp. 288-298.

[11] Wang C, Usami T, Funayama J, Imase F. Low-cycle fatigue testing of extruded aluminium alloy buckling-restrained braces, Engineering Structures, 2013, Vol. 46, pp. 294-301.

[12] Uang CM, Nakashima M, Tsai KC. Research and application of Buckling-Restrained Braced Frames, Steel Structures, 2004, Vol. 4, pp. 301-313.

[13] Xie Q. State of the art of buckling-restrained braces in Asia, Journal of Constructional Steel Research, 2005, Vol. 61, pp. 727-748.

[14] Takeuchi T, Hajjar JF, Matsui R, Nishimoto K, Aiken ID. Local buckling restraint condition for core plates in buckling restrained braces, Journal of constructional steel research, 2010, Vol. 66, pp. 139-149.

[15] Lopez-Almansa F, Castro-Medina JC, Oller S. A numerical model of the structural behavior of buckling-restrained braces, Engineering Structures, 2012, Vol. 41, pp. 108-117.

[16] Zona A, Dall'Asta A. Elastoplastic model for steel buckling-restrained braces, Journal of Constructional Steel Research, 2012, Vol. 68, pp. 118-125.

[17] American Institute of Steel Construction (AISC). Seismic Provisions for Structural Steel Buildings including Supplement, 2005, No. 1, AISC-341.